Practical Coarse Relay Site Planning

Performance Analysis over Composite Fading/Shadowing Channels

Ömer Bulakci · Jyri Hämäläinen · Egon Schulz

Abstract Relay deployments promise to alleviate the limitations of conventional macrocell networks, such as poor indoor penetration and coverage holes in a cost-efficient way. In this context, the capacity of the wireless relay link between a relay node (RN) and its serving base station (BS) has a crucial impact on the end-to-end performance. The deployment flexibility of RNs, which mainly stems from the wireless relay link, compact physical characteristics, and low-power consumption, can be exploited by relay site planning (RSP) to overcome the limitations of the relay link and, thus, enhance the system performance. To this end, RSP is carried out via selecting an RN deployment location from a discrete set of alternatives considering the signal-to-interference-plus-noise ratio (SINR) on the relay link as the selection criterion. In practice, the so-called coarse RSP takes into account only large-scale fading due to shadowing. Nevertheless, as RNs are stationary, the wireless channels pertaining to relay deployments are subject to simultaneous impairments by both shadowing and multi-path fading, i.e., composite fading/shadowing. In this paper, we present the performance of coarse RSP that can be used for planning and dimensioning of two-hop cellular relay networks in composite fading/shadowing environments, where co-channel interference is also present. The relay link is modeled by Nakagami-lognormal distribution while the access link between a mobile terminal (MT) and its serving RN is modeled by Rician-lognormal distribution. Further, we provide an accurate analytical framework through closed-form expressions for relay link SINR, link rates, and end-to-end rate. Results show that coarse RSP can still yield high performance improvements in terms of both SINR and rate considering composite fading/shadowing channels. Moreover, coarse RSP is shown to effectively decrease the amount of fading (AoF) on the relay link and, thus, mitigate the detrimental effects of composite fading/shadowing.

Ö. Bulakci
Huawei European Research Center,
Riesstrasse 25C, 80992 Munich, Germany
E-mail: oemer.bulakci@huawei.com

J. Hämäläinen
Aalto University School of Electrical Engineering, Dept. of Communications and Networking,
P.O.Box 13000, FIN-00076, Espoo, Finland
E-mail: jyri.hamalainen@aalto.fi

E. Schulz
Huawei European Research Center,
Riesstrasse 25C, 80992 Munich, Germany
E-mail: egon.schulz@huawei.com

1 Introduction

Relaying is an integral part of the Fourth Generation (4G) radio access networks, namely, IEEE 802.16m and 3rd generation partnership project (3GPP) long term evolution (LTE) Release 10 and beyond (LTE-Advanced). These two technologies fulfill the requirements of International Mobile Telecommunications Advanced (IMT-Advanced) for 4G radio access networks and, hence, are accorded the official designation of IMT-Advanced [1]. Relay nodes (RNs) promise to increase the network capacity and to better distribute resources in the cell or to extend the cell coverage area [2–5]. Relaying is, as well, regarded a cost-efficient technology. Installing RNs involves lower operational expenditure [6] and provides faster network upgrade when operators aim to improve the quality of service [7]. The cost-efficiency of RNs is further investigated in [8,9].

Inband RNs operate in half-duplex mode to avoid self-interference, i.e., they utilize the same frequency band on both the access link between RN and mobile terminal (MT)

and the relay link between base station (BS) and RN. The performance of inband RNs was investigated in [3]. Therein, it was shown that there is a potential for significant gain if the limitations of the relay link are relaxed. One approach to mitigate such a problem is characterized by relay site planning (RSP), which eludes random deployment of RNs and selects an RN site from a set of different possible locations in order to optimize the relay link quality. We note that according to the discussion on RSP modeling in standardization [10], a certain planning bonus has been added to the relay link channel model in 3GPP evaluation guidelines [11].

Performance evaluation of RSP within LTE-Advanced context was first given in [12]. The study investigated the effect of RSP on the relay link signal-to-interference-plus-noise ratio (SINR) via system-level simulations considering shadowing only. In [13], a basic analytical model for RSP was deduced, where a single dominant interfering BS was considered. Beside the simplified SINR model, the channel model in [13] considers lognormal shadowing on the relay link and Rayleigh fading on the access link. Further, in [14], optimal RSP is analyzed considering composite fading/shadowing (multi-path fading is superimposed on shadowing) and co-channel interference. That is, therein, the maximum achievable gains through site location selection are presented, where the optimal RSP takes into account both shadowing and multi-path fading. Nevertheless, in practice, due to changes in multi-path fading because of, e.g., moving scatterers on the ground, the resultant RSP gains can decrease.

In this paper[1], we build upon the concepts presented in [15] and place the focus on the coarse RSP, which considers only shadowing for site location selection. The corresponding performance is evaluated in composite fading/shadowing environments with co-channel interference. We emphasize that composite fading/shadowing is frequently experienced especially in scenarios with low or no mobility [16, 17]. In addition, given the full-frequency reuse in future cellular networks, co-channel interference is another vital factor to be taken into account for accurate performance analysis. On this basis, we demonstrate the achievable SINR gains on the relay link by the coarse RSP. Though these gains deviate from the maximum achievable levels, results still show a clear gain on the relay link especially when multi-path fading is not severe. Also, the gains translate into higher achieved end-to-end rate provided that the system is not limited by the access link. Another key performance measure in communications over fading channels is amount of fading (AoF), which reflects the severity of the fading [17]. In this work, we show how coarse RSP can effectively de-

crease AoF on the relay link under various channel conditions. Consequently, the performance improvements justify the use of coarse RSP in cellular relay networks.

The remainder of the paper is organized as follows. Section II briefly presents the channel models. In Section III, the modeling of RSP is summarized. In Section IV, the impact of RSP is analyzed along with SINR and rate derivations. Performance results and evaluations are provided in Section V. Finally, Section VI concludes the paper.

2 Channel Models

Shadowing is usually modeled by a lognormal distribution with standard deviation σ and mean μ; σ defines the severity of shadowing. As the parameters of lognormal distribution are often given in decibels, the mappings $\sigma = \lambda \sigma_{dB}$ and $\mu = \lambda \mu_{dB}$ with $\lambda = \ln(10)/10$ can be utilized for the conversion. Besides, the small-scale multipath fading is often characterized by Nakagami distribution with the fading parameter $(0.5 \leq m_{CL} \leq \infty)$ on a communication link (abbreviated by CL in this notation), Rician or Rayleigh distribution. The fading parameter of Nakagami distribution inversely reflects the severity of the multipath fading, i.e., as $m_{CL} \to \infty$ the fading effect diminishes yielding a nonfading channel. Furthermore, Nakagami distribution yields Rayleigh distribution when $m_{CL} = 1$ [16].

The channel models pertain to a two-hop half-duplex decode-and-forward relay deployment where end-to-end performance is degraded also by interference on the relay link. Fig. 1 presents an exemplified schematic of the relay deployment, where a single MT is connected to a single RN A on the access link and is communicating via this RN with a BS A. In this illustration, two neighboring BSs B and C interfere with the serving BS transmission on the relay link. We model the relay and access links by Nakagami-lognormal and Rician-lognormal composite distributions, respectively, which are the two common models in the literature [16–19]. As these composite distributions do not have closed-form expressions, we utilize mixture gamma (MG) distribution [20] to accurately approximate them. It is assumed that interfering signals on the relay link are subject to Rayleigh-lognormal (a.k.a. Suzuki) composite fading/shadowing, as RNs are not expected to have line-of-sight (LOS) links toward interfering BSs. Thus, the total co-channel interference on the relay link is characterized by a sum of Suzuki random variables (RVs). Yet, an exact closed-form expression for the sum of multiple Suzuki RVs is not available, and the Suzuki RVs are *dependent* since in cellular networks shadowing toward different BSs is typically correlated [21]. Further, the SINR derivation becomes cumbersome when the effect of thermal noise is taken into account, and mean received power levels from different interferers

---

[1] Part of this work was presented at the 2013 IEEE Annual International Symposium on Personal, Indoor and Mobile Radio Communications (PIMRC) [15]. In addition to [15], this paper provides a comprehensive analysis and new extensive results.
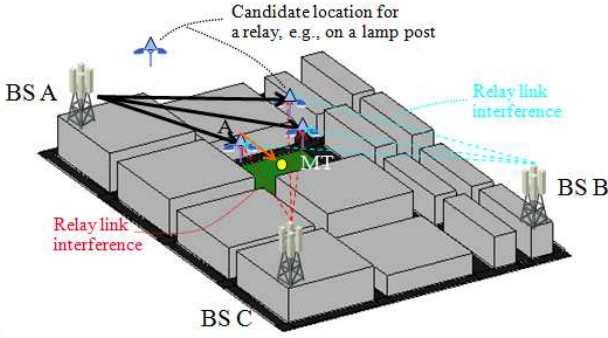
Fig. 1 Exemplified relay deployment and RSP model.

are not equal [22, 23]. Herein, we derive generic SINR distributions addressing such challenges.

In the following, MG distribution is first outlined, and, then, the composite signal-to-noise ratio (SNR) distributions on the relay and access links are modeled in terms of MG distribution [14, 20, 24–26]. The instantaneous SNR and the average SNR are denoted by γ and $\bar{\gamma}$, respectively.

2.1 MG Distribution

The probability distribution function (PDF) of the instantaneous SNR is approximated by MG distribution consisting of N gamma components as [14, 20]

$$f_\gamma(x) = \sum_{i=1}^{N} w_i g_i(x) = \sum_{i=1}^{N} \alpha_i x^{\beta_i - 1} e^{-\zeta_i x}, \quad x \geq 0, \quad (1)$$

where $w_i = \alpha_i \Gamma(\beta_i) \zeta_i^{-\beta_i}$ with $\Gamma(\cdot)$ being the gamma function, $g_i(x) = \zeta_i^{\beta_i} x^{\beta_i - 1} e^{-\zeta_i x} / \Gamma(\beta_i)$ is a standard gamma distribution, and α_i, β_i and ζ_i are the parameters of the ith gamma component. Further, $\alpha_i = \theta_i / C$ where $C = \sum_{i=1}^{N} \theta_i \Gamma(\beta_i) \zeta_i^{-\beta_i}$ is a normalization factor to guarantee that $\sum_{i=1}^{N} w_i = 1$ and $\int_0^\infty f_\gamma(x) = 1$. Accordingly, θ_i is a parameter of the ith gamma component, as well. The number of components N determines the accuracy of the approximation and is obtained by matching the first r (herein, $r = 3$) moments of the approximation and the target distribution [20]. Next, the cumulative distribution function (CDF) of the approximation is given as

$$F_\gamma(x) = \sum_{i=1}^{N} \alpha_i \zeta_i^{-\beta_i} g(\beta_i, \zeta_i x), \quad (2)$$

where $g(a, b) \triangleq \int_0^b t^{a-1} e^{-t} dt$ is the lower incomplete gamma function [27, eq. (8.350.1)].

In addition, the rth moment of MG distribution of the instantaneous SNR is given as

$$E(\gamma^r) = \sum_{i=1}^{N} \alpha_i \Gamma(\beta_i + r) \zeta_i^{-(\beta_i + r)}, \quad (3)$$

where $E(\cdot)$ denotes the statistical expectation. The AoF can be then calculated from the first and the second moments of the SNR as [17]

$$AoF = \frac{\text{var}(\gamma)}{[E(\gamma)]^2} = \frac{E(\gamma^2) - [E(\gamma)]^2}{[E(\gamma)]^2} = \frac{E(\gamma^2)}{[E(\gamma)]^2} - 1, \quad (4)$$

where $\text{var}(\cdot)$ denotes variance.

A key advantage of the MG distribution is the unified framework, i.e., once the parameters of the ith gamma component (θ_i, β_i and ζ_i) are determined, the performance metrics are readily available [20] or can be easily derived.

2.2 SNR Distribution on the Relay Link

The instantaneous SNR on the relay link is modeled by a gamma-lognormal distribution (occurs in Nakagami-lognormal channel) [17, 20]. Then, the parameters of ith gamma component are expressed as [20]

$$\theta_i = \left(\frac{m_{\text{RL}}}{\bar{\gamma}} \right)^{m_{\text{RL}}} \frac{w_i e^{-m_{\text{RL}}(\sqrt{2}\sigma t_i + \mu)}}{\sqrt{\pi} \Gamma(m_{\text{RL}})},$$
$$\beta_i = m_{\text{RL}}, \quad \zeta_i = \frac{m_{\text{RL}}}{\bar{\gamma}} e^{-(\sqrt{2}\sigma t_i + \mu)}, \quad (5)$$

where m_{RL} is the fading parameter of Nakagami distribution on the relay link (abbreviated by RL in this notation), and t_i and w_i are, respectively, abscissas and weight factors of Nth order Hermite integration, and are tabulated for N up to 20 in [28, Table 25.10][2].

The AoF for the SNR distribution on the relay link can be then easily obtained through (3), (4) and (5). A simplified expression of the AoF follows as [30]

$$AoF = \frac{\sqrt{\pi}(m_{\text{RL}} + 1)}{m_{\text{RL}}} \frac{\sum_{i=1}^{N} w_i e^{2\sqrt{2}\sigma t_i}}{\left(\sum_{i=1}^{N} w_i e^{\sqrt{2}\sigma t_i} \right)^2} - 1. \quad (6)$$

2.3 SNR Distribution on the Access Link

An RN cell is typically characterized by small coverage area due to lower transmit power levels relative to the BSs [3, 11]. Accordingly, we assume that a direct LOS component along with many weak non-LOS (NLOS) scatter components exist on the propagation paths between an RN and an MT on the access link. Furthermore, the LOS component may be partially or completely blocked by surrounding objects, e.g., trees, which implies random shadowing [17]. Hence, we model the access link by Rician-lognormal distribution. Accordingly, we obtain the parameters of the ith

---

[2] The abscissas and weight factors can be also generated via various online tools like in [29] for N up to 100.

gamma component [14]:

$$\theta_i = \frac{1+K}{\bar{\gamma}} \left(\frac{m_{\mathrm{AL}}}{m_{\mathrm{AL}}+K} \right)^{m_{\mathrm{AL}}} \frac{(m_{\mathrm{AL}})_{i-1}}{(\Gamma(i))^2} \left(\frac{K(1+K)}{\bar{\gamma}(m_{\mathrm{AL}}+K)} \right)^{i-1}$$

$$\beta_i = i, \quad \zeta_i = \frac{1+K}{\bar{\gamma}}, \tag{7}$$

where $0 \le m_{\mathrm{AL}} \le \infty$ describes the severity of shadowing on the access link (abbreviated by AL in this notation), and $K \triangleq \Omega/2b_0$ is the Rician K factor where Ω is the average power of the LOS component and $2b_0$ is the average power of the scatter component.

The AoF of the SNR distribution on the access link can be deduced using (3), (4) and (7). After some algebraic manipulations, we obtain the simplified AoF expression

$$AoF = \frac{1}{C} \frac{(m_{\mathrm{AL}}+K)^{m_{\mathrm{AL}}-1} K}{m_{\mathrm{AL}}^{m_{\mathrm{AL}}}}$$

$$\times \frac{\sum_{i=1}^{N} \frac{(m_{\mathrm{AL}})_{i-1}\Gamma(i+2)}{(\Gamma(i))^2} \left(\frac{K}{m_{\mathrm{AL}}+K} \right)^i}{\left(\sum_{i=1}^{N} \frac{(m_{\mathrm{AL}})_{i-1}\Gamma(i+1)}{(\Gamma(i))^2} \left(\frac{K}{m_{\mathrm{AL}}+K} \right)^i \right)^2} - 1, \tag{8}$$

where C is the normalization factor as discussed in Section 2.1. It is worth noting that the AoF expressions both on the relay link (6) and access link (8) are independent of the mean SNR $\bar{\gamma}$.

As a reference, the AoF of the original model, which is provided in [17, eq. 2.67], can be obtained by using the transformation $\mathrm{E}(\gamma^r) = \mathrm{E}(\chi^r)A^r$, where $\chi = \gamma/A$ with $A = \frac{\bar{\gamma}}{2b_0+\Omega}$ is the power envelope of the shadowed Rician fading channel, and $\mathrm{E}(\chi^r)$ is given in [17, eq. 2.69]. After some manipulations, the AoF attains the following form

$$AoF = 2 \left(\frac{m_{\mathrm{AL}}+K}{m_{\mathrm{AL}}} \right)^{m_{\mathrm{AL}}}$$

$$\times \frac{{}_2F_1(3, m_{\mathrm{AL}}, 1, K/(m_{\mathrm{AL}}+K))}{({}_2F_1(2, m_{\mathrm{AL}}, 1, K/(m_{\mathrm{AL}}+K)))^2} - 1, \tag{9}$$

where ${}_pF_q(\cdot, \cdot, \cdot, \cdot)$ is the generalized hypergeometric function for integer p and q [27, Sec. 9.14].

3 System Model

3.1 Coarse Relay Site Planning Model

Cell planning and site selection tools are routinely used by operators to improve the system performance and to provide a satisfactory service with minimal deployment expenditure. In this work, it is assumed that the original radio network planning has been done for a single-hop macrocell-only system. Then, RNs are introduced to improve the system performance.

Within the framework of RSP, an RN location is chosen from a set of possible locations. RSP takes into account the channel properties at different locations and considers their links' qualities toward the serving BS in order to enhance the relay link quality. In particular, we assume that there are M potential locations for RN deployment in cell k out of which we select the best location in terms of downlink SINR considering shadowing only. In each location, RN is assumed to be served by a predefined BS solely. Then, the resultant SINR in the selected location is of the following form

$$\Upsilon_{\hat{m},k}^{\mathrm{c}} = \max\{\Upsilon_{m,k}^{\mathrm{c}} : m = 1, 2, ..., M\}, \tag{10}$$

where $\Upsilon_{m,k}^{\mathrm{c}}$ is the SINR for the mth location in the kth cell. We note that while performing coarse RSP, we take into account only shadowing. Thus, the SINR at the selected location $\Upsilon_{\hat{m},k}^{\mathrm{c}}$ can be different that of the actual SINR $\Upsilon_{\hat{m},k}$, which reflects the actual channel conditions impaired by both shadowing and multi-path fading. That is, coarse RSP is carried out based on $\Upsilon_{\hat{m},k}^{\mathrm{c}}$; however, $\Upsilon_{\hat{m},k}$ is the experienced SINR during the operation.

3.2 Multi-cellular Network Model

3.2.1 Network Layout and RSP Location Trellis

The considered network is represented by a regular hexagonal layout with 7 cells, where we look for a suitable location for a single RN in the kth cell assuming M potential location candidates. Fig. 2 depicts the network layout along with the utilized RN location trellis. The RN location trellis models a practical scenario where the $M = 5$ candidate locations are localized in a target region (see also Fig. 1 for a similar scenario with $M = 3$ candidate RN locations). As marked in Fig. 2, d_1 denotes the distance between the serving BS and the midmost RN location. The outer candidate locations are at the same distance of d_2 apart from the midmost candidate location.

3.2.2 Path-loss Model

The path loss, including shadowing, is given by

$$L_{m,k} = \alpha d_{m,k}^{\beta} 10^{\zeta_{m,k}/10}/G, \tag{11}$$

where $d_{m,k}$ the distance between m^{th} potential relay location and k^{th} BS, $k = 0, 1, 2, ..., \mathscr{K}$. Further, α and β are, respectively, a propagation constant and the path-loss exponent, together which define the distance dependent path-loss, G is dimensionless and reflects the impact of antenna gain, which is assumed to be the same for each BS (isotropic antenna gain patterns are employed at BSs). Besides, $\zeta_{m,k}$ is a zero-mean Gaussian random variable (RV) that models the
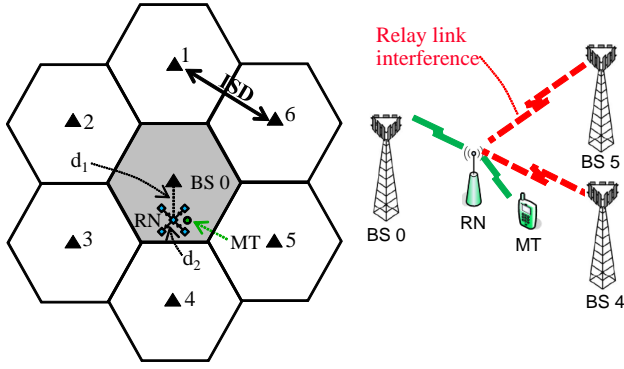
Fig. 2 The network layout and RN location trellis. The distance between two neighboring BSs is the inter-site distance (ISD). The illustration on the right exemplifies the interference caused by BSs 4 and 5 on the relay link.

shadowing. RV $\zeta_{m,k}$ can be expressed as a sum of two independent zero-mean Gaussian RVs ξ_m and $\eta_{m,k}$ with standard deviation of σ_{dB}, where the former corresponds to the near field of the mth location and is the same for all BSs, and the latter variable is a BS-dependent variable, which is independent from one BS to the other [14]. Thus, we have

$$\zeta_{m,k} = \sqrt{\rho} \cdot \xi_m + \sqrt{1-\rho} \cdot \eta_{m,k}, \qquad (12)$$

where ρ is the correlation coefficient related to any pair of BSs. Accordingly, for $k \neq j$, we obtain

$$\mathrm{E}(\zeta_{m,k}\zeta_{m,j}) = \rho\sigma_{dB}^2, \ \mathrm{E}((\zeta_{m,k})^2) = \sigma_{dB}^2, \ \mathrm{E}(\zeta_{m,k}) = 0. \quad (13)$$

That is, shadowing variables $\zeta_{m,k}$ and $\zeta_{m,j}$ are correlated. We note that in 3GPP studies the shadowing correlation coefficient of $\rho = 0.5$ between BSs is usually applied [11].

In accordance with the Gudmundson model [14], the correlation between shadowing samples at different locations in the kth cell is given by

$$\rho(\zeta_{m,k}, \zeta_{n,k}) = e^{-\frac{|d_{m,n}|}{d_{cor}} \ln 2}, \qquad (14)$$

where $\zeta_{m,k}$ and $\zeta_{n,k}$ are the shadowing variables at locations m and n, respectively, $d_{m,n}$ is the distance between the two locations, and d_{cor} is the so-called de-correlation distance. The proposed value for d_{cor} in, e.g., [31], is 20 m. Then, shadowing correlation between potential RN positions with mutual distance of round 50 m, is small and, thus, is neglected in the closed-form analysis. Due to the low correlation in shadowing between candidate locations, the correlation between SINR values is also low and can be ignored.

4 Analysis of Coarse Relay Site Planning

4.1 Derivation of the Actual Relay Link SINR

The actual SINR at the mth location considering composite fading/shadowing is of the following form [14]

$$\Upsilon_{m,k} = \frac{S_{m,k}^2 10^{X_{m,k}/10}}{P_N + \sum_{j \neq k} S_{m,j}^2 10^{X_{m,j}/10}}, \qquad (15)$$

where where $S_{m,k}^2$ is the power envelope of the multi-path fading channel on the desired link between k^{th} BS and m^{th} location, which is modeled by Nakagami distribution, $S_{m,j}^2$ is the power envelope of the multi-path fading channel on the interfering link between j^{th} BS and m^{th} location, which is modeled by Rayleigh distribution, and P_N denotes the thermal noise. Furthermore, $X_{m,k} \sim \mathcal{N}(\mu_{X_{m,k}}, \sigma_{dB}^2)$ with $X_{m,k} = -\zeta_{m,k} + \mu_{X_{m,k}}$ and $X_{m,j} \sim \mathcal{N}(\mu_{X_{m,j}}, \sigma_{dB}^2)$ with $X_{m,j} = -\zeta_{m,j} + \mu_{X_{m,j}}$ are Gaussian RVs, where means $\mu_{X_{m,k}}$ and $\mu_{X_{m,j}}$ comprise BS transmit power levels, and distance dependent path losses defined in (11). As an example, one can easily obtain $\mu_{X_{m,k}} = 10\log_{10}(P_{Tx,k}G\alpha^{-1}d_{m,k}^{-\beta})$ with $P_{Tx,k}$ being the transmit power of the kth BS.

In order to derive an analytically tractable SINR expression, we need to tackle several difficulties. Concretely, an exact closed-form expression for the distribution of the sum of multiple lognormal and/or Suzuki RVs is not available. Moreover, the desired and interfering signals are mutually *dependent* due to shadowing, and there is a constant thermal noise term P_N in the denominator. Substituting (12) along with the aforementioned descriptions of $X_{m,k}$ and $X_{m,j}$ in (15) we obtain

$$\Upsilon_{m,k} = \frac{S_{m,k}^2 10^{(\sqrt{\rho} \cdot \xi_m + \sqrt{1-\rho} \cdot \eta_{m,k} + \mu_{X_{m,k}})/10}}{P_N + \sum_{j \neq k} S_{m,j}^2 10^{(\sqrt{\rho} \cdot \xi_m + \sqrt{1-\rho} \cdot \eta_{m,j} + \mu_{X_{m,j}})/10}}. \qquad (16)$$

Dividing the numerator and denominator by the common shadowing term $10^{\sqrt{\rho} \cdot \xi_m/10}$ yields

$$\Upsilon_{m,k} = \frac{S_{m,k}^2 10^{(\sqrt{1-\rho} \cdot \eta_{m,k} + \mu_{X_{m,k}})/10}}{P_N 10^{-\sqrt{\rho} \cdot \xi_m/10} + \sum_{j \neq k} S_{m,j}^2 10^{(\sqrt{1-\rho} \cdot \eta_{m,j} + \mu_{X_{m,j}})/10}}. \qquad (17)$$

RVs in this re-formulated SINR expression are mutually *independent*. Moreover, the newly introduced RV through thermal noise term $P_N 10^{-\sqrt{\rho} \cdot \xi_m/10}$ follows a lognormal distribution with mean $10\log_{10}(P_N)$ and standard deviation $\sqrt{\rho} \cdot \sigma_{dB}$ in decibels. The sum in the denominator consists of a multiple independent Suzuki RVs and a lognormal RV; therefore, it can be well approximated by a new lognormal RV $10^{0.1Z}$ with $Z \sim \mathcal{N}(\mu_Z, \sigma_Z^2)$ using moment generating

function (MGF)-matching method [14] along with adapted Wilkinson preconditioning [32]. Then, the approximated actual SINR attains the following form of

$$\widetilde{\Upsilon}_{m,k} = S_{m,k}^2 10^{(\sqrt{1-\rho}\cdot\eta_{m,k}-Z+\mu_{X_{m,k}})/10} := S_{m,k}^2 10^{\Delta_{m,k}/10}, \quad (18)$$

where $\Delta_{m,k}$ is a Gaussian RV with mean $\mu_{X_{m,k}} - \mu_Z$ and standard deviation $\sqrt{(1-\rho)\sigma_{\text{dB}}^2 + \sigma_Z^2}$. Accordingly, the actual SINR distribution on the relay link follows a gamma-lognormal composite distribution which is characterized by (1)-(4), where the parameter expressions are provided by (5) in which $\bar{\gamma}$ is set to one.

4.2 Derivation of the Relay Link SINR for Coarse RSP

When only shadowing is considered on the relay link, the SINR formulation in (17) can be re-written as

$$\Upsilon_{m,k}^{\text{c}} = \frac{10^{(\sqrt{1-\rho}\cdot\eta_{m,k}+\mu_{X_{m,k}})/10}}{P_N 10^{-\sqrt{\rho}\cdot\xi_m/10} + \sum_{j\neq k} 10^{(\sqrt{1-\rho}\cdot\eta_{m,j}+\mu_{X_{m,j}})/10}}, \quad (19)$$

where the denominator is a sum of multiple lognormal RVs. Yet, an exact closed-form expression for this sum is not available. In the literature, the most widely used approximation methodology is to represent the sum of independent lognormal variables by another lognormal random variable [32]. Similarly done in Section 4.1, the denominator can be approximated by a new lognormal RV $10^{0.1Z^{\text{c}}}$ with $Z^{\text{c}} \sim \mathcal{N}(\mu_{Z^{\text{c}}}, \sigma_{Z^{\text{c}}}^2)$ using the MGF-matching method along with Wilkinson preconditioning [32]. The resultant SINR reads as

$$\widetilde{\Upsilon}_{m,k}^{\text{c}} = 10^{(\sqrt{1-\rho}\cdot\eta_{m,k}-Z^{\text{c}}+\mu_{X_{m,k}})/10} := 10^{\Delta_{m,k}^{\text{c}}/10}, \quad (20)$$

where $\Delta_{m,k}^{\text{c}}$ is a Gaussian RV with mean $\mu_{X_{m,k}} - \mu_{Z^{\text{c}}}$ and standard deviation $\sqrt{(1-\rho)\sigma_{\text{dB}}^2 + \sigma_{Z^{\text{c}}}^2}$. Accordingly, the resultant SINR distribution on the relay link, which is employed by coarse RSP, follows a lognormal distribution; thus, it is characterized by Gaussian distribution in decibels.

4.3 Maximum Achievable Gains by Optimal RSP

In optimal RSP, the RN location is selected according to the gamma-lognormal composite distribution as provided in (18). Accordingly, when optimal RSP is carried out in the kth cell over M candidate locations, the CDF of the relay link SINR attains the following form[3]

$$F_{\hat{m},k}(\widetilde{\Upsilon}) = \prod_{m=1}^{M} F_{m,k}(\widetilde{\Upsilon}), \quad (21)$$

---

[3] Recall that the variables $\left\{\widetilde{\Upsilon}_{m,k} : m \neq n\right\}$ are assumed to be independent based on the discussion in Section 3.2.2 where uncorrelated shadowing is assumed among the different candidate RN locations.

where $F_{m,k}(\widetilde{\Upsilon})$ is given by (2) following the discussion after (18). Hence, $F_{\hat{m},k}(\widetilde{\Upsilon})$ provides the maximum achievable gains by optimal RSP. On the other hand, the coarse RSP assumes a pure shadowing channel (see Section 4.2) for the RN location selection as given in (10). Consequently, due to multi-path fading component in the selected location $\hat{m}$, the actual SINR may degrade and the associated distribution can deviate from $F_{\hat{m},k}(\widetilde{\Upsilon})$. The PDF is then obtained by taking the derivative of (21) and re-organizing the terms, which yield

$$f_{\hat{m},k}(\widetilde{\Upsilon}) = \left(\prod_{m=1}^{M} F_{m,k}(\widetilde{\Upsilon})\right)\left(\sum_{m=1}^{M} \frac{f_{m,k}(\widetilde{\Upsilon})}{F_{m,k}(\widetilde{\Upsilon})}\right), \quad (22)$$

where $f_{m,k}(\widetilde{\Upsilon})$ is given by (1) following the discussion after (18).

4.4 Impact of RSP on Relay Link AoF

Diversity combining techniques, e.g., maximal-ratio combining (MRC) and selection combining (SC), are routinely used to mitigate the effects of fading and, thus, to enhance the overall received SNR [17,33]. In particular, exploiting different diversity branches, e.g., multiple-receiver antennas, these techniques aim at avoiding the deleterious effect of fading.

Among various widely used diversity combining techniques, SC is relatively less complicated since only one of the diversity branches is processed. Namely, the branch with the highest SNR is selected by the combiner [17]. Accordingly, recalling the RSP model in Section 3.1, we can characterize a simple analogy between SC and RSP. Specifically, in RSP the RN location having the highest SINR is selected which is in analogous to the diversity branch with the highest SINR in SC. Furthermore, the number of RN locations considered in RSP corresponds to the number of diversity branches in SC.

A key performance measure in analysis of RSP is then its impact on the resultant AoF on the relay link. The AoF after RSP can be evaluated[4] using the definition (4) along with the PDF given in (22). Besides, the gain achieved by coarse RSP may decrease relative to optimal RSP as coarse RSP only tackles the impact of shadowing.

4.5 Link and End-to-end Rate Derivations

In the kth cell and at the mth RN location, the relay link rate $R_{r;m,k}$ is given in terms of the relay link SINR as

$$R_{r;m,k} = \delta_r \cdot A_r \cdot \log_2\left(1 + B_r \cdot \widetilde{\Upsilon}_{m,k}\right), \quad (23)$$

---

[4] MATLAB is utilized in AoF evaluations after RSP.
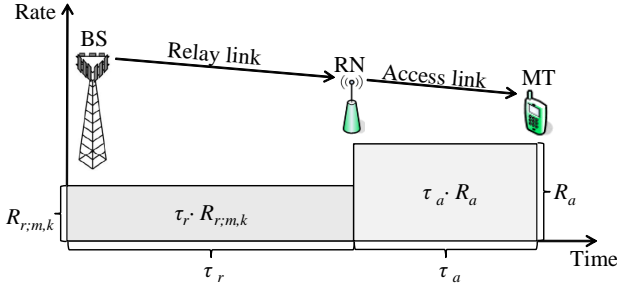
Fig. 3 Example split of resources on the relay and access links.

where A_r and B_r are, respectively, the bandwidth and SINR efficiency factors, and δ_r is the overhead scaling factor which accounts for, e.g., LTE overhead through reference symbols [14]. In case of performing RSP, we obtain the relay link rate $R_{r;\hat{m},k}$ by utilizing the relay link SINR in the selected location, i.e., $\widetilde{\Upsilon}_{\hat{m},k}$. On the other hand, the access link instantaneous rate R_a is of the form

$$R_a = \delta_a \cdot A_a \cdot \log_2\left(1 + B_a \cdot \gamma_a\right), \qquad (24)$$

where γ_a is the instantaneous SNR on the access link, and the parameters A_a, B_a and δ_a may differ from A_r, B_r and δ_r.

The end-to-end rate is, then, given in terms of the rate on the two hops, where due to half-duplex operation, transmissions from BS to RN and from RN to MT are scheduled on different time slots. Fig. 3 exemplifies a resource allocation scheme on the access and relay links. Time resources allocated for the relay link communication constitute τ_r of the total system resources. Similarly, access link communication is scheduled on τ_a of the total available resources, where resource normalization is given as $\tau_r + \tau_a = 1$. Subsequently, the end-to-end rate experienced by a single user served by RN in the kth cell and m^{th} location is defined as the minimum of the user rate achieved on the relay and access links

$$R_{e;m,k} = \min\left(\tau_r \cdot R_{r;m,k}, \tau_a \cdot R_a\right), \qquad (25)$$

where rates on the relay and access links are scaled by the portion of resources allocated to each. When RSP is performed, the end-to-end rate $R_{e;\hat{m},k}$ is formulated similarly considering $R_{r;\hat{m},k}$ instead.

The end-to-end rate, (25), is maximized when the rates on the relay and access links are equal. Then, the optimal resource allocation on the access link and the achieved maximum end-to-end rate are given by

$$\tau_a^{opt} = \frac{R_{r;m,k}}{R_{r;m,k} + R_a}, \qquad (26)$$

$$R_{e;m,k}^{max} = \frac{R_{r;m,k}R_a}{R_{r;m,k} + R_a}. \qquad (27)$$

However, in practice due to resource allocation granularity in time, τ_r or τ_a takes discrete values, e.g., in LTE [11], from the set of $\{0.1, 0.2, \cdots, 0.9\}$.

Table 1 System Parameters

Parameter	Value
General Parameters	
Carrier Frequency	2 GHz
Bandwidth	10 MHz
Frequency Planning	Reuse 1
Duplexing Scheme	Frequency Division Duplex (FDD)
ISD	500 m
RN Location Trellis	d_1=ISD/$\sqrt{3}$ m, d_2=50 m
Bandwidth Efficiencies (A_r, A_a)	0.88
SINR Efficiencies (B_r, B_a)	0.8
Overhead Scaling Factors (δ_r, δ_a)	0.74
Thermal Noise Power Spectral Density (PSD)	-174 dBm/Hz
BS Parameters	
Transmit Power	46 dBm
Antenna Gain	14 dBi
Antenna Configuration and Pattern	Tx-1, Omni-directional
Antenna Height	25 m (above rooftop)
RN Parameters	
Antenna Gain	5 dBi
Antenna Configuration and Pattern	Rx-1, Omni-directional
Antenna Height	5 m (below rooftop)
Noise Figure	5 dB
Shadowing on the Relay Link	
De-correlation Distance (d_{cor})	20 m
Correlation Factor (ρ)	0.5 between cells
Relay Link Path-Loss	
Path-Loss Exponent (β)	3.63
Propagation Constant (α_{dB})	125.2 dB

5 Performance Evaluation

In this section, we evaluate the effect of coarse RSP on the relay link quality and on the end-to-end performance as well as on the resultant AoF on the relay link. Besides, we demonstrate the achievable gains relative to the performance bound. The simulations are conducted using MATLAB as the computational environment. Specifically, 5×10^4-sample Monte Carlo simulations are carried out to ensure reliable statistics. Moreover, the cellular network model as explained in Section 3.2 is implemented in the simulator, where the network layout consists of $\mathcal{K} + 1 = 7$ cells, out of which six neighboring cells cause co-channel interference with the relay-link reception in the midmost cell. In Table 1, the utilized system parameters are summarized in accordance with [11]. Moreover, the simulation models follow the 3GPP guidelines given in [11]. It is worth noting that a good agreement between the utilized analytical models and numerical results is demonstrated in [14]. In addition, we focus on coverage-oriented planning, i.e., RNs are positioned at the cell edge where users experience high interference and/or severe propagation losses toward the serving BS.
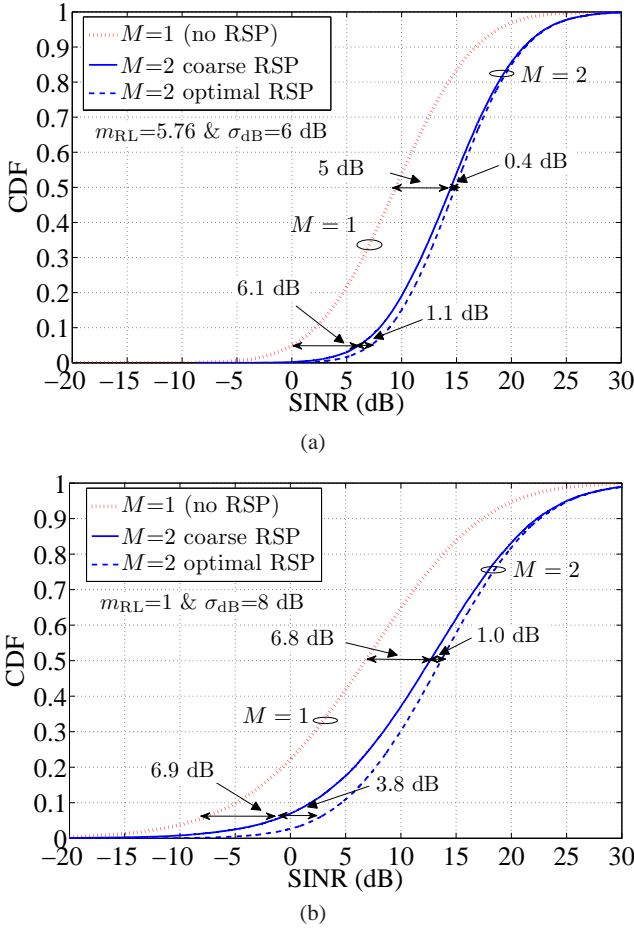
Fig. 4 CDFs of SINR on the relay link with RSP ($M = 2$) and without RSP ($M = 1$). Two sets of channel parameters are depicted; (a) a scenario with comparatively light fading and (b) a scenario with severe fading.

Fig. 5 CDFs of SINR on the relay link with RSP ($M = 5$) and without RSP ($M = 1$). Two sets of channel parameters are depicted; (a) a scenario with comparatively light fading and (b) a scenario with severe fading.

5.1 Relay Link SINR Distribution

The impact of RSP on the relay link SINR distribution is illustrated by CDF plots in Fig. 4 for RSP ($M = 2$) and in Fig. 5 for RSP ($M = 5$). Two sets of channel parameters are considered as:

i) $(m_{RL}; \sigma_{dB}) = (5.76; 6)$ which corresponds to a scenario with comparatively light fading, and

ii) $(m_{RL}; \sigma_{dB}) = (1; 8)$ which corresponds to a scenario with severe fading.

It is noticed that coarse RSP provides high SINR gains especially at lower CDF percentiles in both scenarios. Moreover, it is observed that the gains via coarse RSP deviate less from the maximum achievable gains by optimal RSP in the first scenario particularly at high CDF percentiles. On the other hand, such deviation increases when the impact of multi-path fading becomes more dominant, which is the case in the second scenario. Comparing the different numbers of available candidate locations for RSP, it is seen that the de-

viation between coarse RSP and optimal RSP is less when $M = 2$ and increases when $M = 5$. In addition, the achievable gains through RSP increase as the number of candidate locations increases. For instance, considering the second scenario, coarse RSP with $M = 2$ and $M = 5$ RN candidate locations achieves, respectively, 6.9 dB and 10.4 dB SINR gains at 5%-ile CDF level. It can be as well inferred that as the number of RN candidate locations in RSP increases, the deviation of the SINR CDF plots reduces implying a decrease in the AoF. In the next section, we demonstrate this impact of RSP on the resultant AoF on the relay link. The observed gains through coarse RSP justify its impact in alleviating the effects of severe fading.

5.2 Resultant AoF on the Relay Link

To gain more insight into the impact of RSP, we have plotted in Fig. 6 the AoF values on the relay link as a function of shadowing standard deviation when ($M = 5$). The
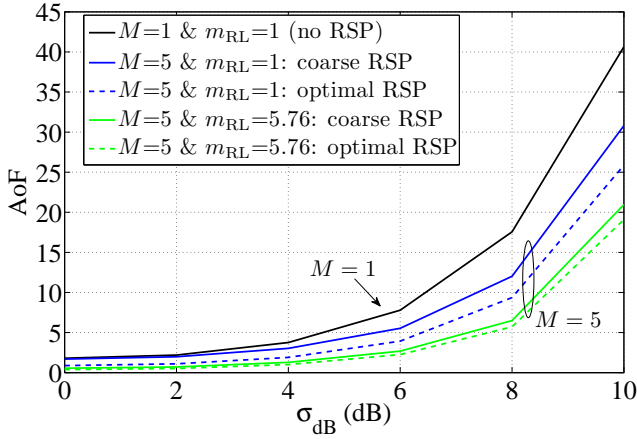
Fig. 6 AoF on the relay link as a function of shadowing standard deviation. The solid lines are obtained by utilizing coarse RSP where $M = 1$ (no RSP) is the reference. The dashed lines are obtained via optimal RSP and illustrate the lower bounds for AoF when utilizing RSP. For $m_{RL} = 5.76$ the multi-path fading is not severe and, hence, shadowing dominates.

case of no RSP ($M = 1$) is taken as a reference. It is seen that AoF on the relay link decreases clearly when coarse RSP is performed and σ_{dB} is large, i.e., heavy shadowing. Thus, Fig. 6 illustrates the effectiveness of coarse RSP in mitigating the deleterious impact of shadowing on the relay link. The lower bounds for AoF when utilizing RSP in Fig. 6 are obtained by utilizing optimal RSP. It is shown that coarse RSP yields similar resultant AoF values as optimal RSP when $m_{RL} = 5.76$ because the multi-path fading is not severe and, hence, shadowing dominates. On the other hand, the deviation between coarse RSP and optimal RSP is more when $m_{RL} = 1$ due to severe multi-path fading. We note that a typical value for the shadowing standard deviation on the relay link is $\sigma_{dB} = 6$ dB, e.g., in the LTE-Advanced standard [11]. Therefore, $\sigma_{dB} = 6$ dB is adopted in what follows.

5.3 Link and End-to-end Rates

Fig. 7 shows the CDFs of the access, relay, and the end-to-end link rates for $M = 5$ (with RSP) and $M = 1$ (no RSP). Two cases are considered for the channel conditions on the access link [14]:

i) frequent heavy shadowing with average access link SNR of $\overline{\gamma}_a = 10$ dB reflects relatively *moderate channel conditions* as shown in Fig. 7(a), while

ii) infrequent light shadowing with average access link SNR of $\overline{\gamma}_a = 20$ dB corresponds to *good channel conditions* as shown in Fig. 7(b).

In both cases, we have $(m_{RL}; \sigma_{dB}) = (5.76; 6)$ and the resource allocation parameters are set as $\tau_r = \tau_a = 0.5$. It can be seen that coarse RSP results in clear rate gain on the relay link relative to no RSP. The deviation from the maximum achiev-

(a)

(b)
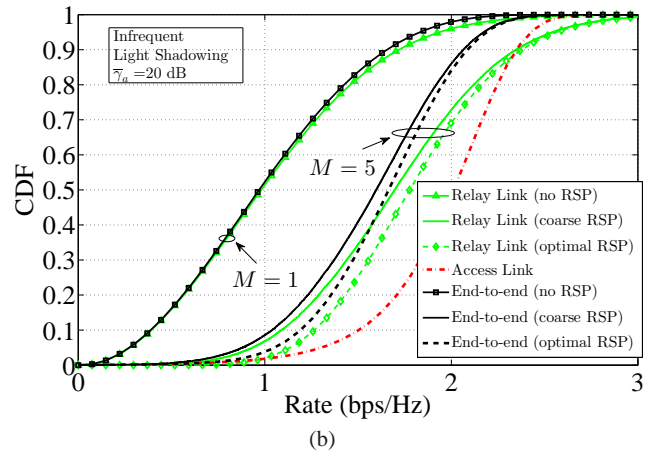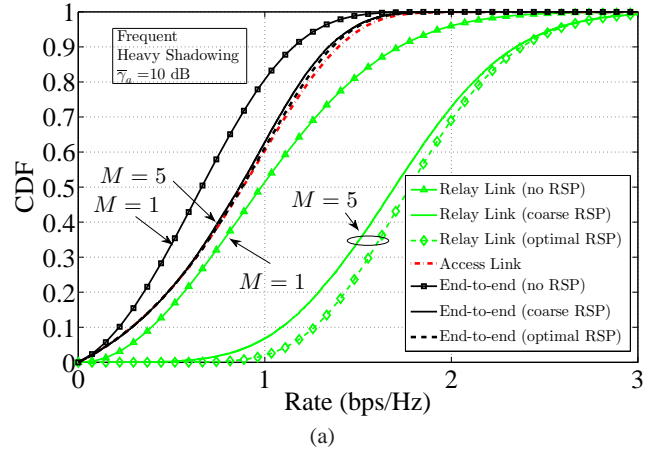
Fig. 7 Relay link, access link and end-to-end rate CDFs when $M = 1$ (no RSP), and when $M = 5$ (with RSP). On the relay link, we have $(m_{RL}; \sigma_{dB}) = (5.76; 6)$. On the access link, (a) moderate channel conditions and (b) good channel conditions are considered.

able SINR gains translates into deviation in rate gains on the relay link, as well. Nevertheless, the end-to-end rate depends on the capacities of both the relay and access links. In this regard, under moderate access link channel conditions, the end-to-end rate performance is limited mainly by the capacity of the access link; the CDF plots of end-to-end and access link rates almost overlap. Therefore, the end-to-end rate performance of coarse RSP is similar to that of optimal RSP at all CDF percentiles. On the other hand, under good access link channel conditions, the end-to-end rate through RSP is, by contrast, limited by the capacity of the relay link. In such a case, the deviation in end-to-end rate performance of coarse RSP from that of optimal RSP becomes notable at lower CDF percentiles. Yet, when performing coarse RSP, a significant gain in end-to-end rate relative to no RSP is still observed.

(a)

(b)
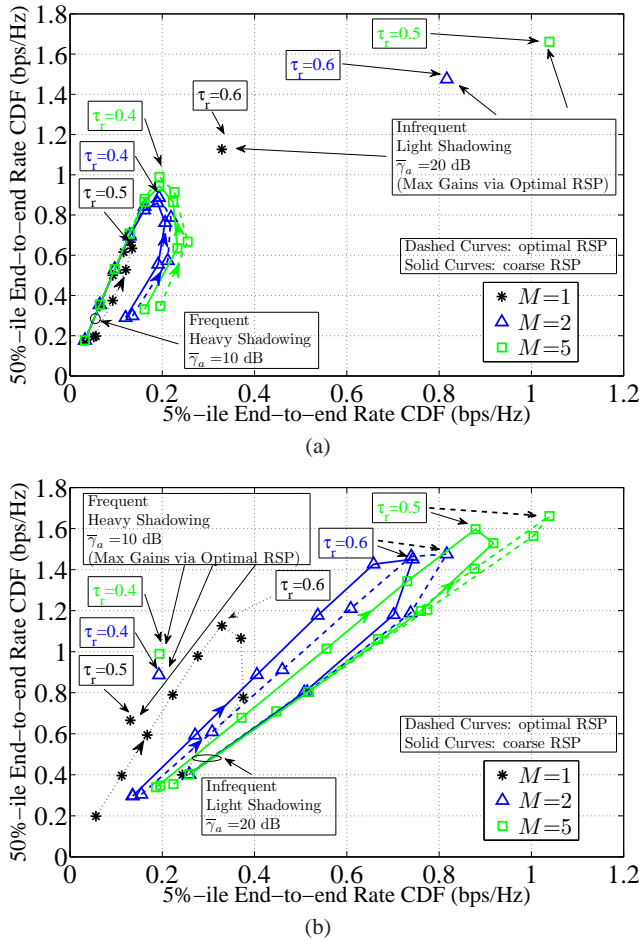
Fig. 8 Achieved 5%-ile versus 50%-ile end-to-end rates for different resource allocation combinations on the access and relay links when $M = 1$ (no RSP) and $M > 1$ (with RSP); (a) moderate access link conditions (b) good access link conditions. The parameter τ_r ranges from 0.1 to 0.9 with a step of 0.1 (each mark indicates a different τ_r). The arrows on the curves indicate the direction of increase in τ_r. Solid and dashed curves correspond to coarse RSP and optimal RSP, respectively.

5.4 Resource Allocation

The optimum resource allocation should take into account the qualities of both relay and access links and balance the achieved rates on them. We consider two performance measures, i.e., the 5%-ile and 50%-ile end-to-end rate CDF levels, and investigate the gains achieved using different resource allocations. We recall that the 5%-ile rate CDF level reflects the cell coverage performance, whereas, the 50%-ile level indicates the median user performance within the cell.

Fig. 8 collectively presents the achieved 5%-ile versus 50%-ile end-to-end rates for a range of relay and access link resource allocation combinations (τ_r, τ_a). Here, τ_r is varied within the range [0.1, 0.9] with a step size 0.1 and $\tau_a = 1 - \tau_r$. In LTE, this step size implies one subframe out of ten potential subframes, equivalently an LTE radio frame. We note that in Fig. 8 different resource allocation combi-

nations (τ_r, τ_a) can be used to maximize either the cell coverage (5%-ile rate CDF level) or the median user performance (indicated by the 50%-ile rate CDF level), or to decide on tradeoff between both criteria. We further note that the increase in the relay link resource allocation is indicated by the direction of the arrows on the curves. In particular, the two cases of channel conditions on the access link analyzed in Section 4.5 are also applied in Fig. 8, where Fig. 8(a) depicts relatively moderate channel conditions and Fig. 8(b) depicts good channel conditions on the access link. Dashed and solid lines correspond to the results of optimal RSP and coarse RSP, respectively, and dotted lines represent the reference scenario of $M = 1$ (no RSP). In both cases of channel conditions, the relay link channel parameters are set as $(m_{RL}; \sigma_{dB}) = (5.76; 6)$. Moreover, for ease of comparison, the operating points yielding the maximum achievable gains via optimal RSP are kept marked in each figure. The results depicted in Fig. 8 point out the importance of the resource allocation for end-to-end rates. That is, a proper resource balance between relay and access links needs to be attained to improve the achieved end-to-end rate gains. Moreover, the 50%-ile and 5%-ile end-to-end rate targets may lead to different optimum resource allocations. In what follows, the gains are determined relative to no RSP with optimum resource allocations maximizing either 5%-ile or 50%-ile end-to-end rates.

In case of moderate access link channel conditions, as shown in Fig. 8(a), since the access link is the bottleneck on the two-hop communications, coarse RSP and optimal RSP yield similar results, see solid and dashed curves. It is seen that coarse RSP with $M = 5$ provides clear gains. For example, the maximum gain of 78% is achieved at 5%-ile end-to-end rate CDF level when $\tau_r = 0.2$, and the maximum gain of 42% is achieved at 50%-ile end-to-end rate CDF level when $\tau_r = 0.4$. Besides, an optimum value of $\tau_r = 0.2$ implies that the access link quality clearly lags behind that of the relay link, see (26). Moreover, it can be seen that due to improvement in relay link quality through coarse RSP, the optimum gains are achieved with reduced resource shares on the relay link. It is also worth noting that when even with only one extra RN candidate location is available, i.e., $M = 2$, significant gains can be achieved.

If access link channel conditions are good, as shown in Fig. 8(b), the relay link quality lags behind the access link quality, e.g., for $M = 1$ (no RSP) the best 5%-ile end-to-end rate is achieved with $\tau_r = 0.8$. In this case, a deviation can be observed between the results of coarse and optimal RSP, see solid and dashed curves. Nevertheless, coarse RSP can still achieve clear gains. For example, in case of performing RSP with $M = 5$, the maximum gain reads as 144% at 5%-ile end-to-end rate CDF level when $\tau_r = 0.6$ and as 42% at 50%-ile end-to-end rate CDF level when $\tau_r = 0.5$. Moreover, similar to the previous case, performing coarse RSP even with

$M = 2$ provides significant gains. Furthermore, with coarse RSP fewer resources are needed on the relay link when maximizing 5%-ile and 50%-ile end-to-end rates. This indicates that the relay link limitations can be eased by coarse RSP yielding better overall end-to-end rates.

6 Conclusion

In this paper, we have investigated coarse RSP as a practical technique to enhance the wireless relay link performance of RNs by exploiting their deployment flexibility. The RN location selection is carried out considering shadowing only, whereas the performance has been analyzed assuming composite fading/shadowing channels. The impact of co-channel interference on the relay link quality is also taken into account within the framework of multi-cellular wireless networks. Moreover, the achievable gains via coarse RSP are demonstrated and compared with the maximum achievable gains by optimal RSP.

Results show that performing coarse RSP still provides significant gains on the relay link SINR relative to no RSP. Besides, AoF is utilized as the performance measure to illustrate the impact of coarse RSP on reducing the severity of fading. It is as well shown that not only does coarse RSP increase median SINR, it also substantially decreases the resultant AoF on the relay link, particularly boosting the low SINR regime. It is seen that coarse RSP deviates less from the maximum achievable gains when the multi-path fading is less severe. Achieved SINR gains on the relay link are shown to translate into clear improvements in end-to-end rates. Further, the deviation from the maximum achievable end-to-end rate gains becomes negligible when the access link is the bottleneck. The importance of balancing resource allocation to realize such gains is illustrated. In particular, it is shown that the 50%-ile and 5%-ile end-to-end rate targets may lead to different optimum resource allocations. It is, as well, illustrated that with coarse RSP fewer resources are needed on the relay link when achieving the optimum end-to-end rates.

References

1. Recommendation ITU-R, "Detailed specifications of the terrestrial radio interfaces of International Mobile Telecommunications Advanced (IMT-Advanced)," ITU-R, Tech. Rep. M.2012, January 2012.

2. R. Schoenen, W. Zirwas, and B. H. Walke, "Capacity and coverage analysis of a 3GPP-LTE multihop deployment scenario," in *IEEE International Conference on Communications Workshops, 2008. ICC Workshops 2008*, Beijing, China, May 2008.

3. A. Bou Saleh, S. Redana, J. Hämäläinen, and B. Raaf, "On the coverage extension and capacity enhancement of inband relay deployments in LTE-Advanced networks," *Journal of Electrical and Computer Engineering*, vol. 2010, pp. 1–12, 2010, article ID 894846.

4. Ö. Bulakci, S. Redana, B. Raaf, and J. Hämäläinen, "Impact of power control optimization on the system performance of relay based LTE-Advanced heterogeneous networks," *Journal of Communications and Networks*, vol. 13, no. 4, pp. 345–359, Aug. 2011.

5. Ö. Bulakci, A. Awada, A. Bou Saleh, S. Redana, and J. Hämäläinen, "Automated uplink power control optimization in LTE-Advanced relay networks," *EURASIP Journal on Wireless Communications and Networking*, vol. 2013, no. 8, pp. 1–19, Jan. 2013.

6. E. Lang, S. Redana, and B. Raaf, "Business impact of relay deployment for coverage extension in 3GPP LTE-Advanced," in *IEEE International Conference on Communications Workshops, 2009. ICC Workshops 2009*, Dresden, Germany, Jun. 2009.

7. K. Doppler, S. Redana, M. Wodczak, P. Rost, and R. Wichman, "Dynamic resource assignment and cooperative relaying in cellular networks: Concept and performance assessment," *EURASIP Journal on Wireless Communications and Networking*, vol. 2009, pp. 1–14, 2009, article ID 475281. [Online]. Available: http://jwcn.eurasipjournals.com/content/2009/1/475281

8. P. Moberg, P. Skillermark, N. Johansson, and A. Furuskar, "Performance and cost evaluation of fixed relay nodes in future wide area cellular networks," in *IEEE 18th Annual International Symposium on Personal, Indoor and Mobile Radio Communications, 2007. PIMRC 2007*, Athens, Greece, Sept. 2007.

9. B. Timus, "Cost analysis issues in a wireless multihop architecture with fixed relays," in *IEEE 61st Vehicular Technology Conference, 2005. VTC 2005-Spring*, Stockholm, Sweden, May 2005.

10. Nokia Siemens Networks (NSN) and Nokia, "Selection criteria for relay site planning," 3GPP Technical Specification Group Radio Access Network Working Group 1, Los Angeles, USA, Tech. Rep. R1-092563, Jun. 2009.

11. Technical Specification Group (TSG) Radio Access Network, "Evolved Universal Terrestrial Radio Access (E-UTRA); Further advancements for E-UTRA physical layer aspects (Release 9)," 3GPP, Tech. Rep. 36.814 v9.0.0, Mar. 2010.

12. Ö. Bulakci, S. Redana, B. Raaf, and J. Hämäläinen, "Performance enhancement in LTE-Advanced relay networks via relay site planning," in *IEEE 71st Vehicular Technology Conference, 2010. VTC 2010-Spring*, Taipei, Taiwan, May 2010.

13. A. Bou Saleh, Ö. Bulakci, J. Hämäläinen, S. Redana, and B. Raaf, "Analysis of the impact of site planning on the performance of relay deployments," *IEEE Transactions on Vehicular Technology*, vol. 61, no. 7, pp. 3139–3150, 2012.

14. Ö. Bulakci, A. Bou Saleh, J. Hämäläinen, and S. Redana, "Performance analysis of relay site planning over composite fading/shadowing channels with co-channel interference," *IEEE Transactions on Vehicular Technology*, vol. 62, no. 4, pp. 1692–1706, 2013.

15. Ö. Bulakci, J. Hämäläinen, and E. Schulz, "Performance of coarse relay site planning in composite fading/shadowing environments," in *IEEE 24th Annual International Symposium on Personal, Indoor and Mobile Radio Communications, 2013. PIMRC 2013*, London, UK, Sept. 2013.

16. G. Stüber, *Principles of mobile communication*. 2nd ed. Kluwer Academic Publishers, MA, USA, 2001.

17. M. Simon and M. Alouini, *Digital communication over fading channels*. 2nd ed. New York: John Wiley & Sons Inc., 2005.

18. A. Abdi, W. Lau, M.-S. Alouini, and M. Kaveh, "A new simple model for land mobile satellite channels: first- and second-order statistics," *Wireless Communications, IEEE Transactions on*, vol. 2, no. 3, pp. 519 – 528, May 2003.

19. J. Paris, "Closed-form expressions for rician shadowed cumulative distribution function," *Electronics Letters*, vol. 46, no. 13, pp. 952 –953, 2010.

20. S. Atapattu, C. Tellambura, and H. Jiang, "A mixture gamma distribution to model the SNR of wireless channels," *Wireless Communications, IEEE Transactions on*, vol. 10, no. 12, pp. 4193 – 4203, Dec. 2011.

21. A. J. Viterbi, A. M. Viterbi, K. Gilhousen, and E. Zehavi, "Soft handoff extends CDMA cell coverage and increases reverse link capacity," *Selected Areas in Communications, IEEE Journal on*, vol. 12, no. 8, pp. 1281 –1288, Oct. 1994.

22. I. Trigui, A. Laourine, S. Affes, and A. Stephenne, "Performance analysis of mobile radio systems over composite fading/shadowing channels with co-located interference," *Wireless Communications, IEEE Transactions on*, vol. 8, no. 7, pp. 3448 –3453, July 2009.

23. I. Petrovic, M. Stefanovic, P. Spalevic, S. Panic, and D. Stefanovic, "Outage analysis of selection diversity over rayleigh fading channels with multiple co-channel interferers," *Telecommunication Systems*, pp. 1–12, 2011. [Online]. Available: http://dx.doi.org/10.1007/s11235-011-9438-z

24. Ö. Bulakci, Z. Ren, C. Zhou, J. Eichinger, P. Fertl, and S. Stanczak, "Dynamic nomadic node selection for performance enhancement in composite fading/shadowing environments," in *IEEE Vehicular Technology Conference, 2014. VTC 2014-Spring*, Seoul, South Korea, May 2014, pp. 1–5.

25. W. Cheng, "Performance analysis and comparison of dual-hop amplify-and-forward relaying over mixture gamma and generalized-k fading channels," in *IEEE Wireless Communications & Signal Processing (WCSP), 2013 International Conference on*, 2013, pp. 1–6.

26. S. Mukherjee, *Analytical Modeling of Heterogeneous Cellular Networks*. Cambridge University Press, 2014.

27. I. Gradshteyn and I. Ryzhik, *Table of Integrals, Series and Products*. 7th ed. Academic Press Inc., 2007.

28. M. Abramowitz and I. Stegun, *Handbook of mathematical functions with formulas, graphs, and mathematical tables*. Dover publications, 1964.

29. Casio. (2012) Nodes and weights of Gauss-Hermite. [Online]. Available: http://keisan.casio.com/has10/SpecExec.cgi?id= system/2006/1281195844

30. S. Atapattu, C. Tellambura, and H. Jiang, "Representation of composite fading and shadowing distributions by using mixtures of gamma distributions," in *Wireless Communications and Networking Conference (WCNC), 2010 IEEE*, April 2010, pp. 1 –5.

31. Broadband Wireless Access Working Group, "Multi-hop relay system evaluation methodology (channel model and performance metric)," IEEE 802.16m, Tech. Rep. 06/013r3, Feb. 2007. [Online]. Available: http://www.ieee802.org/16/relay/docs/ 80216j-06_013r3.pdf

32. Ö. Bulakci, J. Hämäläinen, A. Bou Saleh, S. Redana, and B. Raaf, "Impact of preconditioning on the convergence of numerical co-channel interference approximations in heterogeneous networks," in *Wireless Communications and Mobile Computing Conference (IWCMC), 2011 IEEE 7th International*, July 2011, pp. 119 –124.

33. P. Shankar, "Performance analysis of diversity combining algorithms in shadowed fading channels," *Wireless Personal Communications*, vol. 37, no. 1, pp. 61–72, 2006.